Mathematical Modelling and Analysis
Volume 15 Number 2, 2010, pages 245–255
Doi:10.3846/1392-6292.2010.15.245-255

ISSN 1392-6292 print
ISSN 1648-3510 online
www.vgtu.lt/mma/

An Algorithm for Partitioning of Right Heart Ventricle Medial Axis

M. Paulinas and M. Meilūnas

Vilnius Gediminas Technical University
Saulėtekio al.11 LT-10223, Vilnius, Lithuania
E-mail(*corresp.*): mantas.paulinas@el.vgtu.lt
E-mail: mm@fm.vgtu.lt

Received September 21, 2009; revised March 03, 2010; published online April 20, 2010

Abstract. A right heart ventricle has a complex and irregular shape, this obscures analysis of ventricle surface movements. We are trying to quantitative evaluate morphological changes of right ventricle surface, these changes appear during heart beat cycle, between different age groups, due to heart diseases, and other factors. A method for such evaluation would open new possibilities for insights into heart function, disease course extrapolation and other. We see this as a multistage task, where the first step is partitioning whole surface into smaller, more manageable regions, and the second step is to analyse each region separately. In this paper we present a new algorithm for partitioning the medial axis of right heart ventricle surface. Such partitioning leads to division of surface into smaller regions with clear shape. The proposed algorithm first computes medial axis from sampled ventricle surface. Later, the medial axis is filtered and smoothed, and third, we compute curvature map and use it as weights in Dijkstra's algorithm for curvature guided partitioning. Algorithm provides a way for fully automatic partitioning of medial manifold into separate medial scaffolds and a semi automatic way for additional curvature based division of medial scaffolds.

Keywords: mathematical modelling, medial axis, partitioning, heart ventricle, symmetry sheet.

AMS Subject Classification: 65D18.

1 Introduction

The human heart is a complex muscular organ, it contains four main chambers: two ventricles and two atriums. They form two pumping units, which move blood. Left unit pumps blood to aorta and to whole body and right unit takes deoxygenated blood and moves it to lungs for oxygen refill. The left ventricle has a simple shape, most of it's cross sections in the direction of a long heart axis are circular. This allows easily calculate volumetric properties (capacity,

blood flux, etc.) using the disk method, i.e. the area of each cross section is multiplied by distance between two cross sections. The right ventricle, in contrary to the left one, has a complex shape which is difficult to see from two-dimensional echocardiography images due to restrictions of possible cross sections. The complex shape causes troubles while evaluating ventricle's volumetric properties. To make it easer, we are trying to reconstruct right ventricle surface and it's movement from echocardiographic images, namely from three or four cross sections. To achieve this we need a way to quantitavely evaluate morphological changes of the right ventricle surface. These changes appear during heart beat cycle, between different age groups, due to heart diseases, etc. Such knowledge would allow to improve surface reconstruction, besides that it would open new possibilities for insights into heart function, disease course extrapolation, etc. There were some attempts to reconstruct right ventricle from a couple of cross sections as described in [13], but their method was based on the assumption that contours intersect perpendicularly, which is not the case in clinical practice. They have interpolated the whole ventricle surface using only the shape of contours, the possible influence of certain features of contour to the whole shape was not considered.

For the analysis of biological structures various methods are available, i.e., principal components analysis for mean shape construction and analysis of variations from it (see, [15]), or parametrisation using spherical harmonics and their coefficient analysis [9]. We want to capture small changes in surface, as well as big changes in object, for this we chose medial axis (MA) transform [1] of segmented right ventricle images. The definition of a medial axis is given in Section 2.1. Several unique advantages of using medial axis or skeleton to model geometric objects are described in [8]. Good overview of available techniques for MA extraction is provided by Giblin and Kimia in [10].

Despite the wide range of techniques available for the computation of the medial axis, its usefulness in real-world applications has been limited mainly because of the complex structure in three-dimensional space, also due to the fact that it is constructed from intersecting sheets of symmetry (medial scaffolds). We note, that the topological structure of the medial axis has not been effectively captured in a graph format. Giblin and Kimia [10] analyse construction of medial axis and define five different types of entities, which in turn are organized into points, curves and sheets. Besides that, they propose a theoretical background for 3D medial axis shape description by using hyper-graph notation [10].

For a thorough analysis of the right heart ventricle surface and its medial axis we need to simplify this general method. We try to partition it into two dimensional medial scaffolds – 2D sheets in 3D space. They would allow a simplified analysis and parametrisation of ventricle surface.

2 Algorithm

Our proposed algorithm uses multi-step approach. During the first step, medial axis is computed from a sampled ventricle surface. The computation is performed using algorithm proposed by Dey [7] which approximates MA as a

sub-complex of Voronoi diagram.

During the second step MA is partitioned into separate symmetry sheets, which may still have complex shapes. To divide them into smaller and simpler shapes, during the third step we compute curvature maps for every sheet, and use them as weights for Dijkstra's algorithm which in turn computes shortest dividing paths on MA sheets.

2.1 Computation of medial axis

The true medial axis for the first time was defined by Blum in [1]. We use another definition by Dey [5] which states that the medial axis of a curve (surface) $F \subset \mathbb{R}^k$ is the closure of the set of points in $\mathbb{R}^k$ that have at least two closest points in F.

Different approaches of MA computation exist, our choice of particular approach was based on initial data we have. It is manually segmented CT scans of human heart. The scans capture right ventricle region as well as temporal information during heart movement. One heart beat cycle is captured in ten three-dimensional images with voxel size $0.39 \times 0.39 \times 5$ mm.

Low number of spatial samples limits application of voxel based medial axis extraction techniques and lead to a geometric medial axis approximation. It is approximated from surface samples and is computed according to the algorithm described in [7]. It is shown in [6] that if surface sampling density approaches infinity, then the medial axis approximation approaches true medial axis.

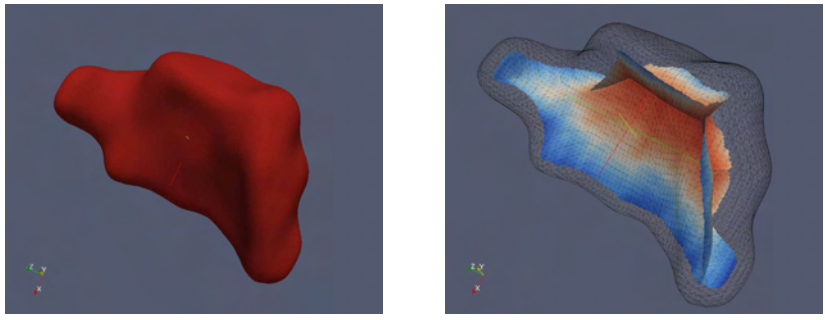

a) b)

Figure 1. The right heart ventricle a) reconstruction from up sampled and smoothed image data; b) medial axis with superimposed mesh wire frame.

We note that an important condition is to have a sufficient surface sampling. In order to obtain a dense and uniform surface sampling, we have tried to approximate the surface by using spherical harmonics, as described in [14]. But such approximation introduces additional high frequency components on surface, which in turn produces additional sheets in medial axis. The obtained results led us to a simpler solution: up-sample and smooth out initial data, and use some scalar field contouring algorithm (such as marching cubes [12]) on it. This produces smooth surfaces and reasonably dense sample points (see Fig. 1a).

The mesh produced by a scalar contouring algorithm can't be used for further computation, it is not guaranteed that the produced surface samples triangulation is equivalent to Delaunay triangulation and is dual to a Voronoi diagram as required by the algorithm. The MA extraction algorithm begins with computation of Delaunay triangulation of the mesh vertices and extraction of specific data structures–umbrellas [7]. It is a collection of surface polygons having one common point and forming a topological disk (see Fig. 2a). Umbrellas extraction from Delaunay triangulation is done by using complementary cone (co-cone) concept [4]. Co-cone is a double cone surface (Fig. 2b), which pinch point coincides with surface sample, and this sample defines a Voronoi cell. Co-cone axis passes through the surface sample and through the farthest Voronoi cell vertex p^+.

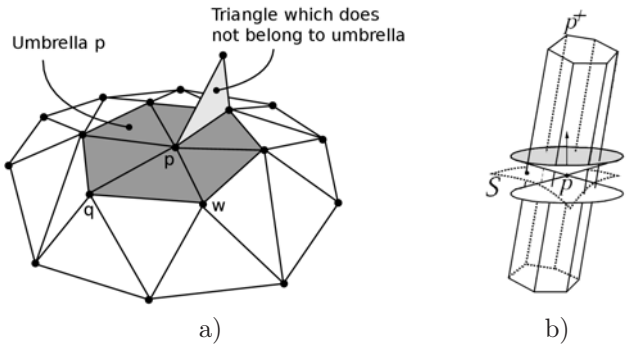

Figure 2. a) Umbrella – surface polygons, that share one common point and form a topological disk; b) complementary cone and it's position in space with respect to Voronoi cell and surface, here p^+ the farthest Voronoi cell vertex [4].

The Voronoi diagram is filtered using angle and ratio criterions, complete explanation of the criterions can be found in [5]. Filtering prunes most of the Voronoi diagram faces, leaving only those satisfying both criterions. Remaining set of Voronoi faces approximate medial axis, as depicted in Fig. 1b. The faces are convex polygons with varying number of vertices. To simplify further analysis we triangulate all faces and obtain a mesh which is composed from triangles. Using this algorithm one may still run into problems near sharp corners, even if the sampling is sufficiently dense. Near sharp corners sampling density requirement approaches infinity and lead to errors of MA approximation. In our case, heart is composed from soft tissues and do not contain sharp features, thus, infinite sampling density problem is not encountered.

2.2 Initial partitioning of medial axis

We adopt a naming and subdivision conventions proposed by Giblin and Kimia in [10]. They define five basic entities that compose medial axis:

- A symmetry sheet, which is denoted by A_1^2.

- Intersection of locally three (globally it might be only two sheets as shown in Fig. 3) symmetry sheets produce a curve and it is denoted by A_1^3.
- Besides this curve, open symmetry sheet edge form a curve too, it is denoted by A_3.
- The point at which curves A_1^3 and A_3 meet, is denoted by A_1A_3.
- In some special cases, four symmetry sheets meet at one point, this point is denoted A_1^4.

Described entities are shown in Fig. 3. Further details on them can be found in the original article.

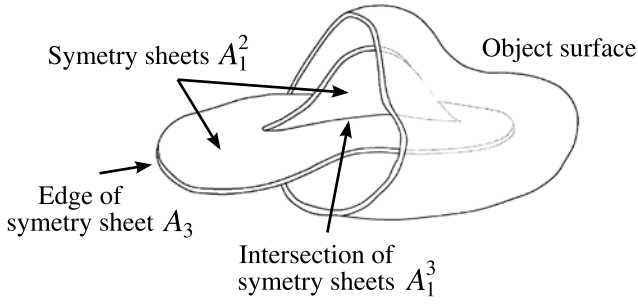

Figure 3. Main medial axis entities: A_3 is the edge of symmetry sheet, A_1^3 is the intersection of symmetry sheets, A_1^2 is the symmetry sheet.

A computed medial axis is approximated by convex polygons, which where subdivided into triangles, thus the whole MA surface is composed from triangles. It consists of surface sample points p_i, which are connected by edges $e_k = (p_i, p_j)$, where $k = 1, 2, \ldots, n$ and triplets of edges form surface faces f_i. Each edge connects two surface samples and possibly fully or partially approximates A_1^3 or A_3 curve. One edge may represent the whole curve, or the curve can be composed from series of edges. We assume that, if a set contains faces, then it contains edges and surface samples which define faces as well.

Each edge has one or more neighbouring faces. Let $n_f(e_k)$ be a function which gives a number of neighbouring faces for edge e_k. On the approximated MA, we define A_3 curve as a series of connected edges, which are adjacent to one and only one face, $A_{S3} = \{e_k : n_f(e_k) = 1\}$. A_{S1}^3 curve is defined as a series of edges which have three neighbouring faces, $A_{S1}^3 = \{e_k : n_f(e_k) = 3\}$. Interior of symmetry sheet is composed from surface samples connected by edges, which have two neighbouring faces. All the sheet samples are bounded by A_1^3 and A_3 curves, thus open sheet boundary is composed from edges adjacent to one face, and boundary at sheets intersection is composed from edges adjacent to three faces.

Initial partitioning labels each MA surface sample, and shows to which MA entity the sample belongs. We start by dividing all edges into three sets: A_1^e,

A_2^e and A_3^e, where $A_k^e = \{\forall e_k \in A_k^e : n_f(e_k) = k\}$. Edges in the first set belong to open boundaries, the second set contains edges belonging to MA interior and the third set contains intersections of medial sheets.

To create a curve A_1 approximating edge sequence C_n^1, as a starting point we take any edge from A_1^e and start an iterative procedure. Collect all directly neighbouring edges and check each edge membership in set A_1^e, if it does belong to A_1^e then it belongs to the curve. The edge is added to the set C_n^1 and removed from A_1^e. Collection procedure is repeated until none of collected neighbouring edges are present in A_1^e or two edges with ending points of type A_1A_3 are collected, they mark two ends of the curve. The collection procedure spreads in two directions along edge curve, after collecting edge with A_1A_3 end point, spreading in that direction should stop.

After the stopping criterion is met and curve is constructed, another edge should be selected as a starting point, and edge collection procedure repeated, thus constructing another open boundary curve. The procedure should be repeated until the set A_1^e is not empty.

To produce A_1^3 curves approximating sequences C_n^3, the same procedure is used. Set A_1^e is replaced by A_3^e, and curves may finish with A_1A_3 or A_1^4 points.

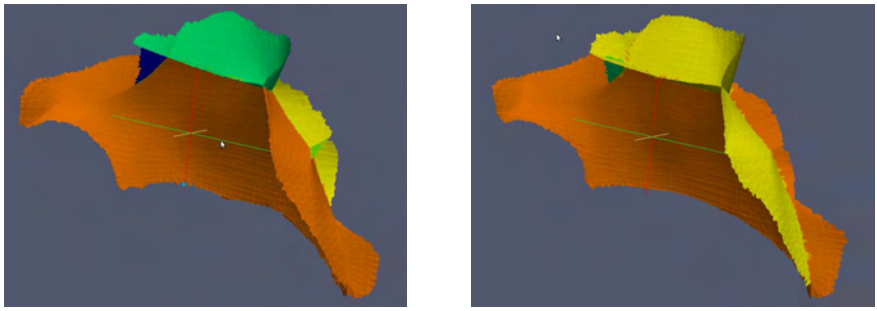

a) b)

Figure 4. Partitioned medial axis in different time moments of heart beat. In a) there is more separated sheets than in b).

To construct a set of medial sheet samples first we need to define a set C which is union of all C_n^1 and C_n^3 sets, and a set M which holds whole medial axis. The construction of a medial sheet S_n starts by selection of one sample point p_i from M which is not a member of C and adding it to a temporary set Ω. For all samples in Ω collect all direct neighbours (samples which share one edge with p_i) to a set N and check each member of N whether it belongs to C or S_n, or not. If it does, then it is a boundary point or an already visited point, we do not need to analyse its neighbours, we remove it from N, and if it is a boundary point, then we add it to S_n. Move all points from Ω to S_n and from N to Ω. Repeat neighbours collection again until Ω becomes empty, then the set S_n is constructed and contains all medial sheet interior and boundary points.

The subdivided medial axis is shown in Fig. 4a. Different shades mark different symmetry sheets. As can be seen in Fig. 4a, symmetry sheets of the

right heart ventricle are quite complicated in shape. During the heart beat, it's shape changes and it's medial axis changes. Symmetry sheets connect and disconnect, appear and disappear during different phases of a beat cycle (see, Fig. 4a and b). During one phase medial axis is composed from separate sheets, while during the other phase some of the sheets get connected. It was observed that at the places where symmetry sheets connect, there are higher curvature ridges.

To avoid the instability problem and to partition medial axis into simpler shapes we add another step, which tries to divide symmetry sheets on high curvature ridges.

2.3 Curvature guided partitioning of Medial Axis

The sheets of medial axis are two-dimensional structures embedded into three-dimensional space. Each sheet may be curled and twisted, thus forming a complex shape in three dimensional space. To simplify them, we perform additional subdivisions by tracing paths on sheet surface. We have observed several data sets and found that symmetry sheets can be divided at higher curvature ridges. Smaller parts should be bounded by sheet boundaries and ridges.

MA mesh can be seen as a hyper-graph with nodes at mesh vertices, then divided paths become paths in a graph. For them we use Dijkstra's shortest path in graph algorithm (see [3]). It computes shortest paths from one fixed node to all remaining graph nodes.

To subdivide one symmetry sheet we perform iterative procedure, where several dividing paths may be computed. We assume that every subdividing curve should start at points where A_3 and A_1^3 curves meet and it can end either at a similar point or at any open boundary point. We denote the set of ending points by T and the set of starting points by P.

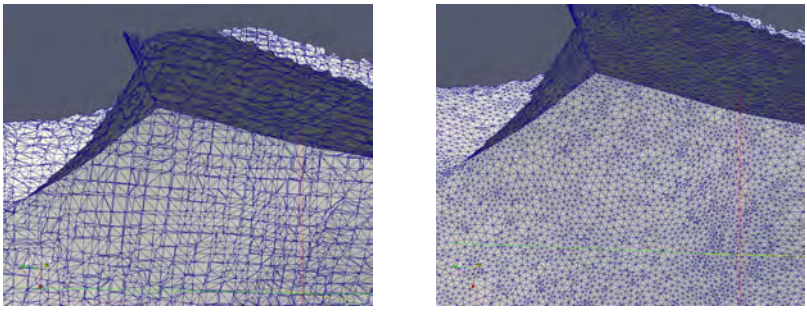

a) b)

Figure 5. Laplacian filtering of medial axi: a) before filtering, b) after filtering.

To make shortest paths follow curvature ridges, we compute Gaussian curvature at every vertex of the MA. To take into account different sizes of faces, we add additional weight to each face's contribution in curvature computation, $w_f = A(f)/3$.

To improve computation of the curvature we need a way to smooth a mesh.

For this one can use sophisticated methods such as solving non linear diffusion equation, as it is used for images [2]. Such equations are solved in different ways as in [11] and are computationally expensive, but they keep small features in a mesh. For our purposes we chose a simple Laplacian smoothing on medial axis mesh, it improves uniformity of the mesh (see Fig. 5). The smoothing operation is defined as $p_i^s = \frac{1}{N}\sum_{j=1}^{N} p_j^{s-1}$, where N is the number of neighbouring vertices which are directly connected to p_i and s is the number of iteration. At each iteration the mesh is relaxed. To minimize distortions of the boundary contours, during smoothing operation all boundary vertices remains fixed and are not moved. For smoothing we have used up to 20 iterations.

Paths on the MA are computed from all members of P to all members of T, then shortest path is selected for each starting point. Every obtained shortest path is a new dividing curve for the symmetry sheet. The computation is performed on whole MA and every sheet is used. To avoid jumps from one sheet to another, we assign infinite weights to all points of A_1^3 curves and use weighted computation of shortest paths.

We note, that after cycling over all possible source and target points, we obtain additional subdivisions for symmetry sheets.

3 Results

The provided algorithm subdivides MA in two steps. First, initial partitions are found, where each partition represents one symmetry sheet and can have a quite complex shape. In order to simplify this shape, the algorithm tries to compute additional dividing paths. Each path is traced along higher curvature ridges, and the algorithm connects one A_1A_3 point with another A_1A_3 point, or with some different type point which lies on an open sheet boundary.

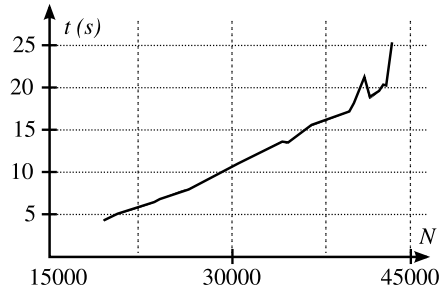

Figure 6. Computation times in seconds for differently sized medial axes. N is the number of points in approximated medial axis.

Computation times for initial partitioning are provided in Fig. 6. In the given range the computation time almost linearly depends on the number of points in the medial axis. The sizes of all analyzed medial axes fall into the given range. The sudden jump at the right part of the graph can be explained by a shortage of the fast memory of the computer, and usage of swap.

Timing of computation of dividing paths cannot be directly related to the

number of points in MA. It also depends on the number of points in open boundaries, and on the number of A_1A_3 points, so it depends on configuration of MA and on the number of points in it. Another strong factor for timing of the whole procedure is a required manual adjustment of target points. Overall processing of one medial axis, including extraction, filtering and points adjustment takes from 5 to 10 minutes. This makes from 1 to 2 hours for one heart dataset composed from 10 temporal images. All computations were performed on a machine with single core, 3 GHz processor and 2 GB of random access memory.

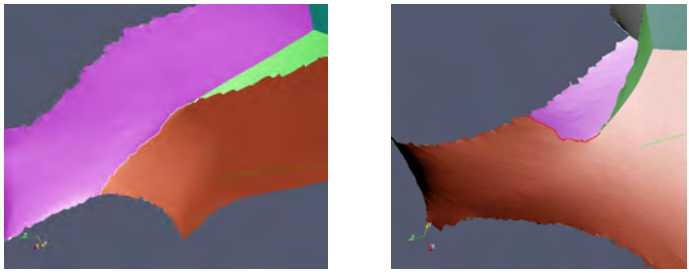

a) b)

Figure 7. Subdivision of symmetry sheet obtained at two different time moments.

During experiments we have observed, that the shortest path on symmetry sheet, not necessarily is the best way to subdivide the sheet. Sometimes, especially if a source point is located close to the open boundary, the shortest path isn't the best choice as can be seen in Fig. 7b. In such cases the target points should be selected manually and the dividing paths recalculated. Fig. 8 shows the initial subdivision and curvature based subdivision with manual adjustment, the subdivided MA is clearly composed from simple shaped sheets.

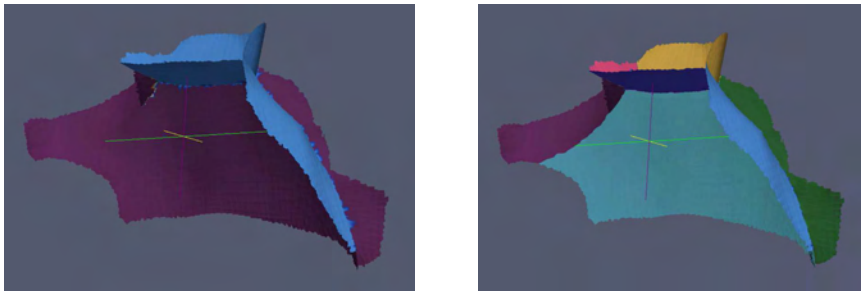

a) b)

Figure 8. Initial subdivision after first step and final subdivision after second step.

Fig. 9 shows how subdividing curve connects to medial sheets, which were connected at one time moment and were disconnected on another. This information can be used to track surface features in time if they split into several parts.

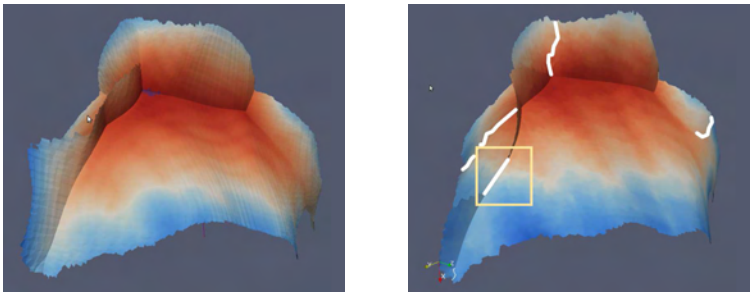

a) b)

Figure 9. Medial axis at different time moments. Subdivision curve connects two medial sheets, which where connected before (lines were enhanced for better visibility).

For additional partitioning it is possible to try a recursive subdivision approach, which possibly could lead to even simpler parts of MA and this could be advantageous for more complex shapes. If the results are to be used for surface parametrisation, recursive subdivision may introduce separation of regions which span the MA partition.

4 Discussion

The proposed semi-automatic medial axis partitioning method subdivides medial axis into simpler shapes. They represent parts of the object surface and can be used for its analysis or surface subdivision, i.e., surface is subdivided in accordance to parts of MA, the surface points are connected with points on MA. The new parts of the surface will be symmetric with respect to the medial axis and simpler in their shape. Simplicity of the shape facilitates the surface parametrisation task.

It is possible to extend this algorithm with recursive subdivision, such a modification can be beneficial for analysis of very complex shapes. The extension would require thorough analysis of recursive subdivision process to determine the stopping conditions and evaluate obtained small patches of the medial axis. Uncontrolled recursive subdivision would possibly lead to a meaningless structure.

For a better automation of the described algorithm, point tracking in time can be used. It would allow to track points of MA in time and keep them stable, thus minimizing number of manual adjustments.

Surface subdivision into small patches, with respect to medial axis partitions, and their parametrisation facilitates analysis of surface motion in time. Analysis of medial axis symmetry sheets and their partitions might reveal interesting information about the movement of surface features and their evolution during different time points. It opens a possibility for measurement of surface morphological changes in time, and enables a better surface approximation where interpolation is needed.

References

[1] H. Blum. A transformation for extracting new descriptors of shape. In Weiant Wathen-Dunn(Ed.), *Models for the Perception of Speech and Visual Form*, pp. 362–380, Cambridge, 1967. MIT Press.

[2] R. Čiegis, A. Jakušev, A. Krylovas and O. Suboč. Parallel algorithms for solution of nonlinear diffusion problems in image smoothing. *Math. Model. Anal.*, **10**(2):155–172, 2005.

[3] T. H. Cormen, C. E. Leiserson and R. L. Rivest. *Introduction to algorithms.* MIT Press, Cambridge, MA, USA, 2001. ISBN 0-262-03293-7.

[4] T. K. Dey and S. Goswami. Tight cocone: a water-tight surface reconstructor. In *SM '03: Proceedings of the eighth ACM symposium on Solid modeling and applications*, pp. 127–134, New York, NY, USA, 2003. ACM. ISBN 1-58113-706-0. Doi:10.1145/781606.781627.

[5] T.K. Dey. *Curve and Surface Reconstruction: Algorithms with Mathematical Analysis (Cambridge Monographs on Applied and Computational Mathematics).* Cambridge University Press, 2006.

[6] T.K. Dey and W. Zhao. Approximating the medial axis from the Voronoi diagram with a convergence guarantee. *Algorithmica*, **38**(1):179–200, 2003. ISSN 0178-4617. Doi:10.1007/s00453-003-1049-y.

[7] T.K. Dey and W. Zhao. Approximate medial axis as a Voronoi subcomplex. *Computer-Aided design*, **36**(2):195–202, 2004. Doi:10.1016/S0010-4485(03)00061-7.

[8] H. Du and H. Qin. Medial axis extraction and shape manipulation of solid objects using parabolic PDEs. In *SM 04: Proceedings of the ninth ACM symposium on Solid modeling and applications*, pp. 25–35, 2004.

[9] G. Gerig, M. Styner, D. Jones, D. Weinberger and J. Lieberman. Shape analysis of Brain Ventricles using SPHARM. *Mathematical Methods in Biomedical Image Analysis, IEEE Workshop on*, **0**:171, 2001. Doi:10.1109/MMBIA.2001.991731.

[10] P. Giblin and B.B. Kimia. A formal classification of 3D medial axis points and their local geometry. *IEEE Trans. Pattern Anal. Mach. Intell.*, **26**(2):238–251, 2004. ISSN 0162-8828. Doi:10.1109/TPAMI.2004.1262192.

[11] A. Handlovicova and Z. Kriva. Perona-Malik equation – error estimates for explicit finite volume scheme. *Math. Model. Anal.*, **10**(4):353–366, 2005.

[12] W.E. Lorensen and H.E. Cline. Marching cubes: A high resolution 3d surface construction algorithm. In *SIGGRAPH '87: Proceedings of the 14th annual conference on Computer graphics and interactive techniques*, pp. 163–169, New York, NY, USA, 1987. ACM. ISBN 0-89791-227-6. Doi:10.1145/37401.37422.

[13] L. Mockus, M. Meilūnas, M. Paulinas, A. Ušinskas and D. Zakarkaitė. Generating of reformat slices in neural and cardio-tomography. *Math. Model. Anal.*, **12**(1):121–130, 2007.

[14] M. Paulinas and J. Rokicki. Methodology for computation and filtering of medial axis of similar surfaces. In *Proceedings of internation converence on biomedical engineering*, pp. 209–212, 2008. (In Lithuanian)

[15] M. Rychlik, W. Stankiewicz and M. Morzynski. Applications of 3D PCA method for extraction of mean shape and geometrical features of biological objects set. *Math. Model. Anal.*, **13**(3):413–420, 2008. Doi:10.3846/1392-6292.2008.13.413-420.